Journal of Structural Biology xxx (2017) xxx–xxx

Contents lists available at ScienceDirect

Journal of Structural Biology

journal homepage: www.elsevier.com/locate/yjsbi

The structure of the "amorphous" matrix of keratins

Murat Kadir [a], Xinwei Wang [b], Bowen Zhu [b], Jing Liu [b], Duane Harland [c], Crisan Popescu [d,*]

[a] Lubrizol Advanced Materials, Inc., 9911 Brecksville Road, Brecksville, OH 44141, USA
[b] Department of Mechanical Engineering, 2025 Black Engineering Building, Iowa State University, Ames, IA 50011, USA
[c] AgResearch Limited, Lincoln Research Centre, Private Bag 4749, Christchurch 8140, New Zealand
[d] KAO Germany GmbH, Pfungstädterstr. 98-100, D-64297 Darmstadt, Germany

ARTICLE INFO

Article history:
Received 12 November 2016
Received in revised form 31 March 2017
Accepted 1 April 2017
Available online xxxx

Keywords:
Keratin
Matrix
Phonon
Spin-diffusion
Transmission electron microscopy

ABSTRACT

Various keratin fibers, particularly human hairs, were investigated by transmission electron microscopy, TEM, solid-state ^{1}H NMR and Transient Electro-Thermal Technique, TET. The results converge to suggest that the matrix of keratin fiber cortex, far from being amorphous, has a well-defined nano-scale grainy structure, the size of these grains being around 2–4 nm. The size of the grains appears to strongly depend on the chemical treatment of the fiber, on the temperature and on the relative humidity of the environment, as well as on the physiological factors at the level of fiber production in follicle.

By suggesting an organization at the nano-scale of the protein chains in these grains, likely to be Keratin Associated Proteins, the results challenge the view of matrix as a homogeneous glassy material. Moreover, they indicate the potential of further investigating the purpose of this structure that appears to reflect not only chemical treatments of keratins but also biological processes at the level of the follicle.

1. Introduction

Trichokeratins are a key protein constituent of the mammalian solution to the need for hard, lightweight and chemically resistant structures, e.g., hairs, claws, hooves and horns (Wang et al., 2016; Popescu and Hoecker, 2007). Different from other fibrous proteins (Schrooyen et al., 2000), such as collagen, elastin and myofibrillar proteins, trichokeratin (or hard keratin) normally provides outer covering and protection of organisms due to the large amount of disulfide bonds (Trabbic and Yager, 1998) and a unique three-dimensional structure (Zhao et al., 2003; Lynch et al., 1986).

Hard keratin structures, wool and human hair in particular, have been historically well studied for industrial reasons. The *meso*-structure of the fibril-matrix composite as established using X-ray and electron-based methods is summarized in Fig. 1.

In a very simplistic way one may depict keratin materials as being composed of keratin intermediate filaments, KIF, surrounded by the matrix (dark area between KIFs in Fig. 1). A more detailed description takes into account also the existence of an interface between KIFs and surrounding matrix, formed of heads and tails of the filaments protruding and connecting into matrix, as well as of other ionic and covalent bonds between side aminoacids of filaments and surrounding matrix (Istrate et al., 2013). While the KIFs are known from a bulk of experimental data to be well organized, crystalline structures (Fraser et al., 1964), the matrix is largely assumed as an amorphous material gluing the filaments and the interface phase is considered as being a very thin layer of the size of a bond length.

The present work aims at challenging the view of matrix as a homogeneous glassy material by investigating its nano-structure for accessing details which may reveal protein organization at that scale. It also looks at how various chemical treatments affect this organization.

2. Experimental

2.1. TEM

For transmission electron microscopy, New Zealand Romney mid-side wool fibers were scoured with detergent (Teric GN9) and then heptane, air dried and mounted across an acetate frame as in earlier studies (Harland et al., 2011b). Quills from African crested porcupine (*Hystrix cristata*) were also chosen based on observations that compared to other quills those from *H. cristata* have a particularly regular internal structure in X-ray diffraction experiments (Parry and Fraser, 2015). Individual quills were washed in water and cut into small transverse or longitudinal strips, avoiding the medulla. Strips were mounted on acetate

* Corresponding author.
E-mail addresses: murat.kadir@lubrizol.com (M. Kadir), xwang3@iastate.edu (X. Wang), duane.harland@agresearch.co.nz (D. Harland), crisan.popescu@kao.com (C. Popescu).

http://dx.doi.org/10.1016/j.jsb.2017.04.001
1047-8477/

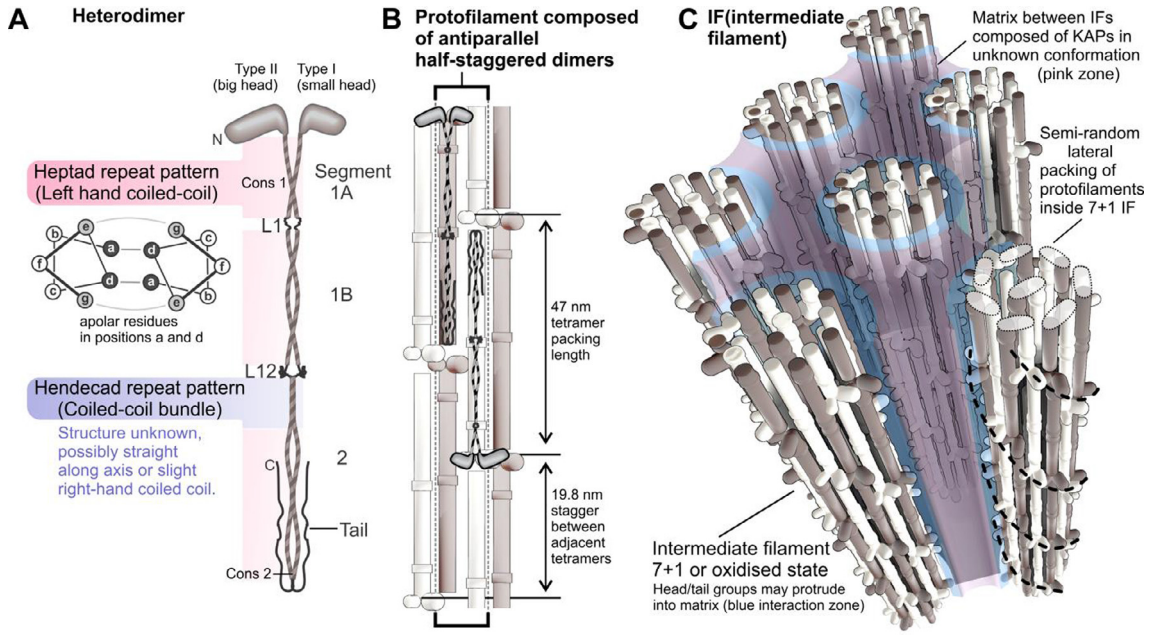

Fig. 1. Keratin fiber structure as it is currently understood. **A**. Heterodimers of Type I and Type II keratin are held in a rod-like conformation by heptad and hendecad coiled-coil segments interrupted by two flexible linkers (Smith et al., 2002; Parry, 2006; Chernyatina et al., 2015). Head and tail segments contain only local regions of structural regularity, but likely play a part in stable filament assembly. **B**. Dimers within a filament form tetramers composed of antiparallel dimers which stack longitudinally, we assume here an A11 or A22 oxidized state (Fraser and Parry, 2005). **C**. Keratin intermediate filaments are composed of seven tetramers that spiral longitudinally with one tetramer trapped internally. The lateral organization of the tetramers is slightly random (Er Rafik et al., 2004). Most head groups, and possibly tails may interact with the protein matrix in which filaments are embedded, with this interaction region having different chemo-physical properties than the rest of the matrix (Istrate et al., 2013) which is composed of keratin-associated proteins (KAPs). **Key**: Cons, consensus sequence; IF, keratin intermediate filament; L1 and L12 are linkers.

frames. Mounted samples were air dried before being placed in four changes of LR White acrylic resin (2 h × 2 and overnight on rotator) and polymerized for 19 h at 60 °C.

Sections cut (Ultracut UCT, Leica, Germany; 35° diamond knife, Diatome, Switzerland) at 100 nm onto copper grids with no support film were examined at 250 kV using a FEI (USA) Tecnai T3 TEM with Compustage to determine optimal sample thickness for tomography. 100 nm sections of Porcupine quill on 700 mesh hexagonal grids were selected. Comparison porcupine quill and wool cortex in some samples was made after section staining (uranyl acetate and lead citrate) using at 80 kV (FEI Morgagni 268D). Comparison of both of these samples were also made with Romney wool samples stained using 3 cycle reduction osmication as described in (Harland et al., 2011a).

For cryo-TEM and stain-free electron tomography, samples were coated at high vacuum with 2 nm carbon (Edwards E306A, Edwards High Vacuum, UK) and examined at 200 kV using a JEOL (Japan) JEM-2200FS Cryo-TEM with micrographs captured by a TVIPS-TemCam F416 (TVIPS-GmbH, Germany), and both controlled by Serial EM 3.4 software (University of Colorado, USA).

Tilt series were collected at 40,000× microscope magnification (pixel width 0.312 nm). For dry and hydrated samples both low-dose (focus on adjacent areas) and the energy filter were used to maximize the contrast and reduce sample degradation. Only transversely cut samples proved to reconstruct well enough to be used. Tomograms were reconstructed and examined using the IMOD 4.5.7 software suite (University of Colorado, USA).

For observation of hydrated sections using cryo-TEM, sections were placed on a 5 μL drop of distilled water for 10 min, removed, excess water wicked off with a filter paper and 15 nm gold fiducially applied in a 10% dilution droplet (5 μL) for 3 min. Excess liquid was wicked off and grid was immediately plunge frozen in liquid-nitrogen cooled ethane (Leica, KF80). Grids were stored under liquid nitrogen until examined.

Analysis of tomograms was carried out using IMOD and micrographs using AnalySIS Five (Olympus Imaging Systems, Germany). A mixture of image enhancement and spatial frequency tools were used to examine differences in low contrast images. Fast Fourier transforms were used to locate regions of micrographs and tomograms with high levels of structural spacing at around 8–11 nm, corresponding to the expected filament spacing. A few filaments were then located visually using virtual projections of full thickness (~80 nm) and by moving up and down through the tomogram using a virtual projection integrated from 16 to 30 slices. Many earlier electron microscopy and X-ray based studies have established that trichokeratin KIFs in their final state are close to 7.6 nm diameter. Likely boundaries of the filaments were determined by looking for circular patterns of this diameter. While many isolated filaments were found this way, further examination was given to the few regions where multiple circles were found in close proximity. Thresholding was then used to identify blobs of higher local electron density within and between the fitted 7.6 nm circles using single slices (0.31 nm thick). Further analysis was not possible due to the data quality and uncertainty over artifacts possibly caused by electron damage, the imaging and reconstruction process.

2.2. NMR

Merino wool fibers and genetically Caucasian origin (Western Europe, Brown, Eumelanin type) human scalp hair fibers. All fibers were cleaned by water washing and dried freely under controlled environmental conditions (55% relative humidity and 25 °C) before being used for further examinations. Proton solid state NMR spectra, ^{1}H double-quantum (DQ) build-up curves, ^{1}H spin diffusion, and ^{13}C CPMAS spectra were measured on a Bruker DSX-500 spectrometer operating at 500.45 and 125.84 MHz for ^{1}H and ^{13}C, respectively.

Please cite this article in press as: Kadir, M., et al. The structure of the "amorphous" matrix of keratins. J. Struct. Biol. (2017), http://dx.doi.org/10.1016/j.jsb.2017.04.001